Big Bang Nucleosynthesis constraints on resonant DM annihilations

An update to ACROPOLIS

Pieter Braat
Work together with Marco Hufnagel
Theory seminar Oslo

Nikhef

University of Amsterdam

The Netherlands (“the Low Lands”)



The Netherlands (“the Low Lands”)



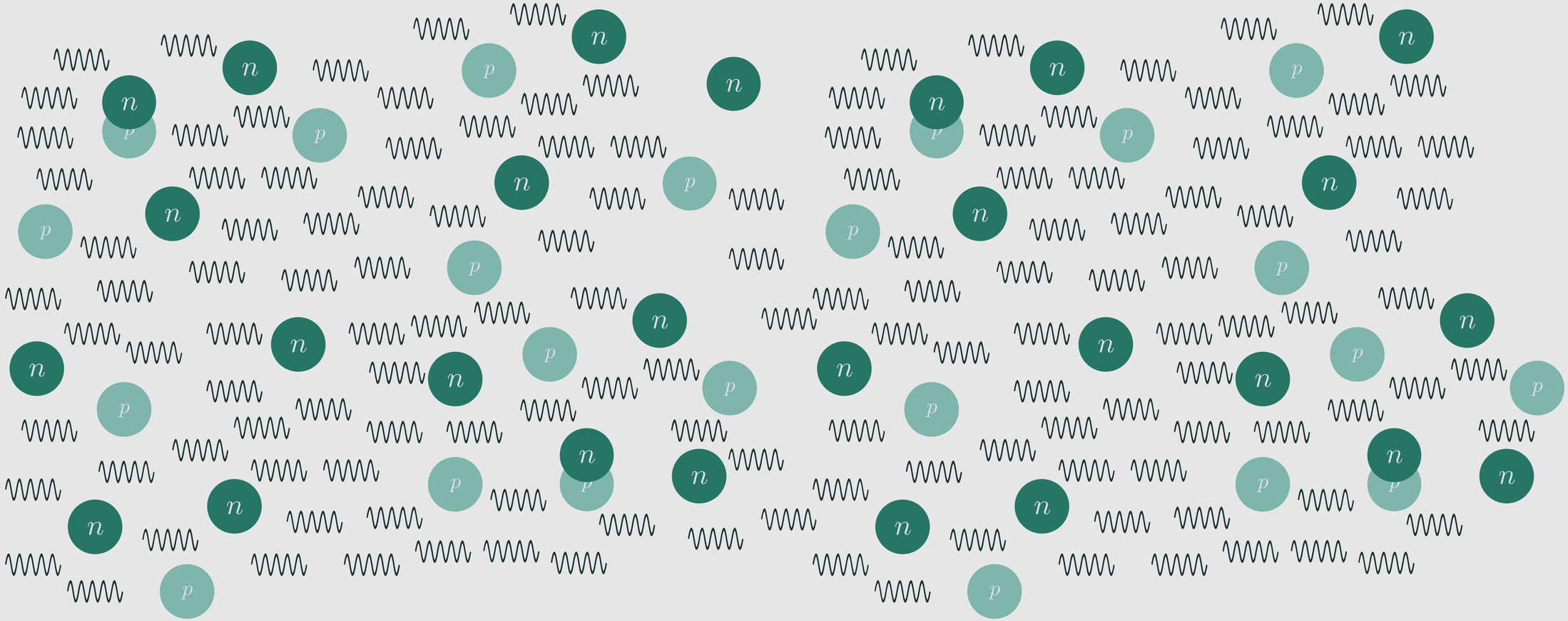
Oslo (not so low lands)

Big Bang Nucleosynthesis

Big Bang Nucleosynthesis 101

or: primordial light element formation in a nutshell*

$$n + p \rightleftarrows D + \gamma$$



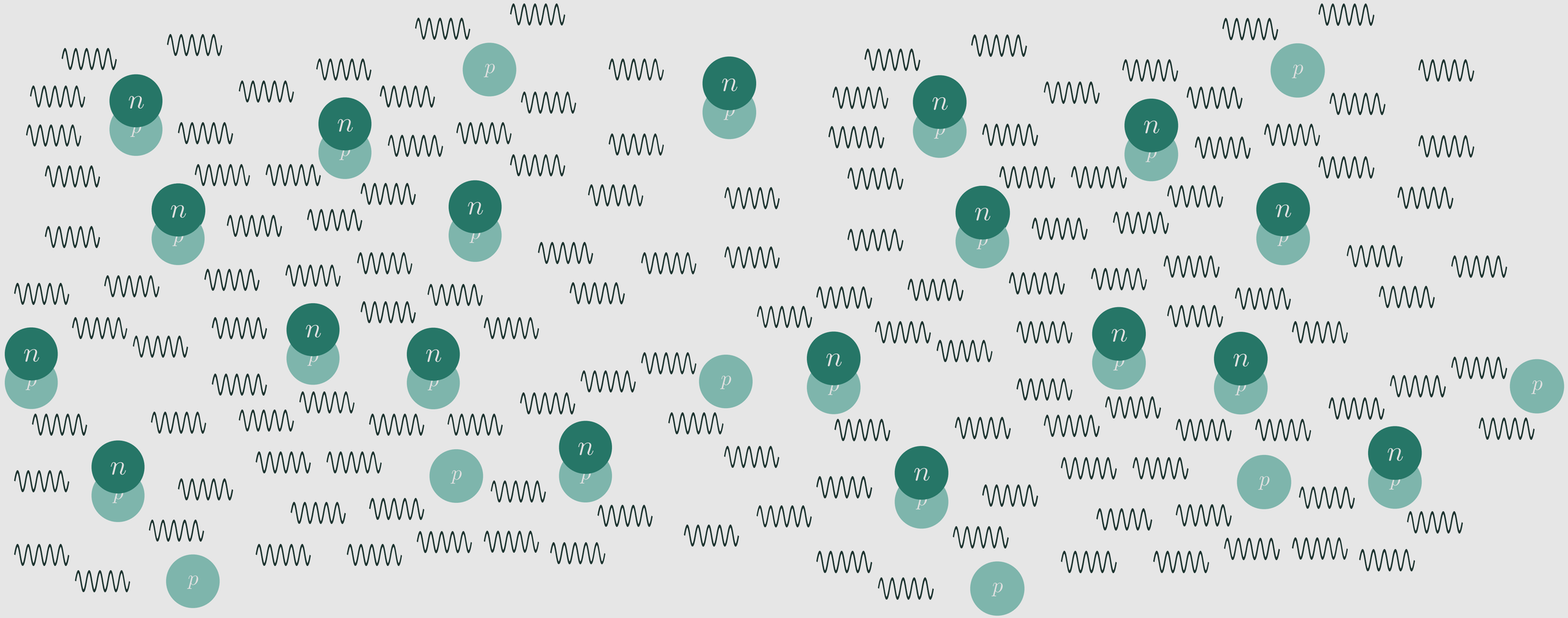
$$T > 1\,\mathrm{MeV}$$

*# of particles not to scale

Big Bang Nucleosynthesis 101

or: primordial light element formation in a nutshell*

$$n + p \rightleftarrows D + \gamma$$



$$T \sim 1 \text{ MeV}$$

*# of particles not to scale

Big Bang Nucleosynthesis 101

or: primordial light element formation in a nutshell*

$$n + p \rightleftarrows D + \gamma$$



$$T \sim 1 \text{ MeV}$$

*# of particles not to scale

Big Bang Nucleosynthesis 102

or: primordial light element formation in a nutshell

Combining input from nuclear/particle physics and cosmology,
we can predict the abundances quite precisely

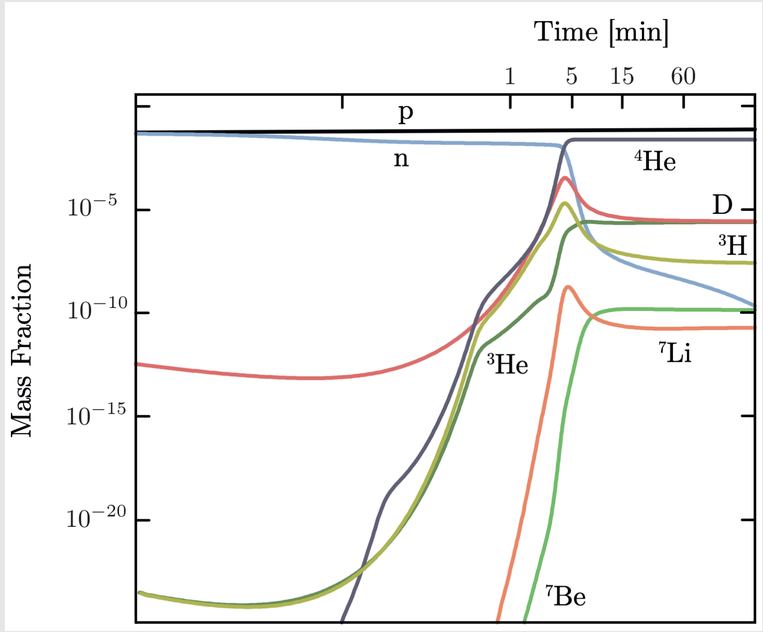


Figure taken from Baumann *Cosmology*

E.g. Helium-4 mass fraction $\mathcal{Y}_p \equiv \frac{\rho(^4\mathrm{He})}{\rho(^1\mathrm{H})} \sim \frac{1}{4}$

Big Bang Nucleosynthesis 102

or: primordial light element formation in a nutshell

Combining input from nuclear/particle physics and cosmology, we can predict the abundances quite precisely

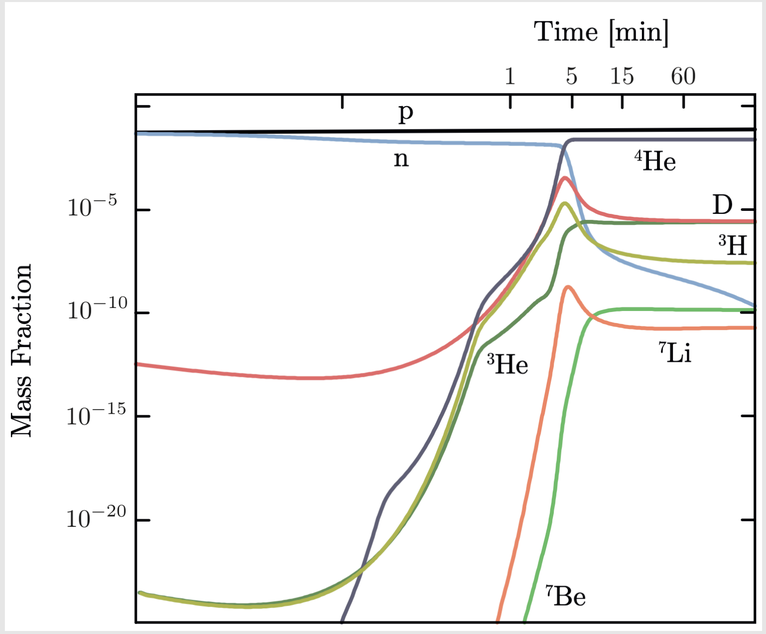


Figure taken from Baumann *Cosmology*

E.g. Helium-4 mass fraction $\mathcal{Y}_p \equiv \frac{\rho(^4\mathrm{He})}{\rho(^1\mathrm{H})} \sim \frac{1}{4}$

Observations from primordial gas clouds



$$\mathcal{Y}_p = 0.245 \pm 0.003$$

$$\mathrm{D}/^1\mathrm{H} = (25.47 \pm 0.25) \times 10^{-6}$$

PDG (2022)

$\Rightarrow$ Can use observations to constrain new physics

Photodisintegration

Probe of BSM physics

Can use the observations of lightest elements to constrain BSM physics:

BSM physics during BBN:

- Existence of new light degrees of freedom $m_\chi \gtrsim 10\,\mathrm{MeV}$ (thermal relic)
- Changes to the fundamental coupling constants $G_F, \alpha_{EM}, \ldots$

Or after BBN: photodisintegration

Probe of BSM physics

Can use the observations of lightest elements to constrain BSM physics:

BSM physics during BBN:

- Existence of new light degrees of freedom $m_\chi \gtrsim 10\,\mathrm{MeV}$ (thermal relic)
- Changes to the fundamental coupling constants $G_F, \alpha_{EM}, \ldots$

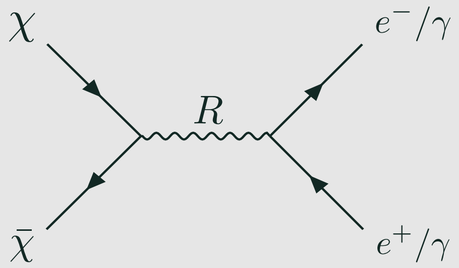
Or after BBN: photodisintegration

Exotic EM energy injection (from BSM Physics) can destroy the newly formed elements





e.g. DM annihilations $\chi\bar{\chi} \to e^- e^+/\gamma\gamma$



Photodisintegration window

Light element abundances $N \in \{n, p, \mathrm{D}, {}^3\mathrm{H}, {}^3\mathrm{He}, {}^4\mathrm{He}, {}^7\mathrm{Li}, {}^7\mathrm{Be}\}$

Photodisintegration is sensitive to specific temperature range

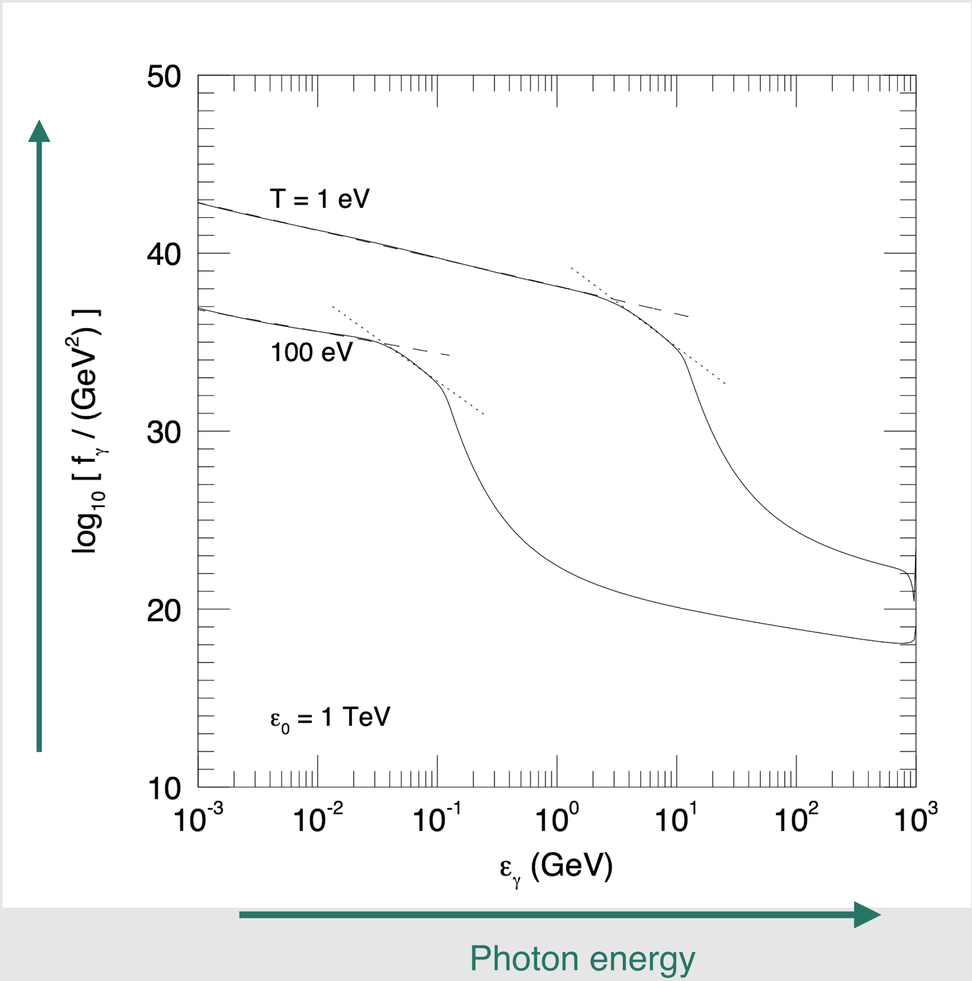
At early times highly energetic photons are rapidly depleted from pair creation

$$\gamma\gamma_{\mathrm{th}} \to e^+e^-$$

~ # photons

Temperature threshold is

$$E^{\mathrm{th}}_{e^+e^-} \simeq \frac{m_e^2}{22T}$$



from Kawasaki and Moroi (1995) [astro-ph/9412055]

Photodisintegration window

Light element abundances $N \in \{n, p, \mathrm{D}, {}^3\mathrm{H}, {}^3\mathrm{He}, {}^4\mathrm{He}, {}^7\mathrm{Li}, {}^7\mathrm{Be}\}$

Photodisintegration is sensitive to specific temperature range

At early times highly energetic photons are rapidly depleted from pair creation

$$\gamma\gamma_{\mathrm{th}} \to e^+e^-$$

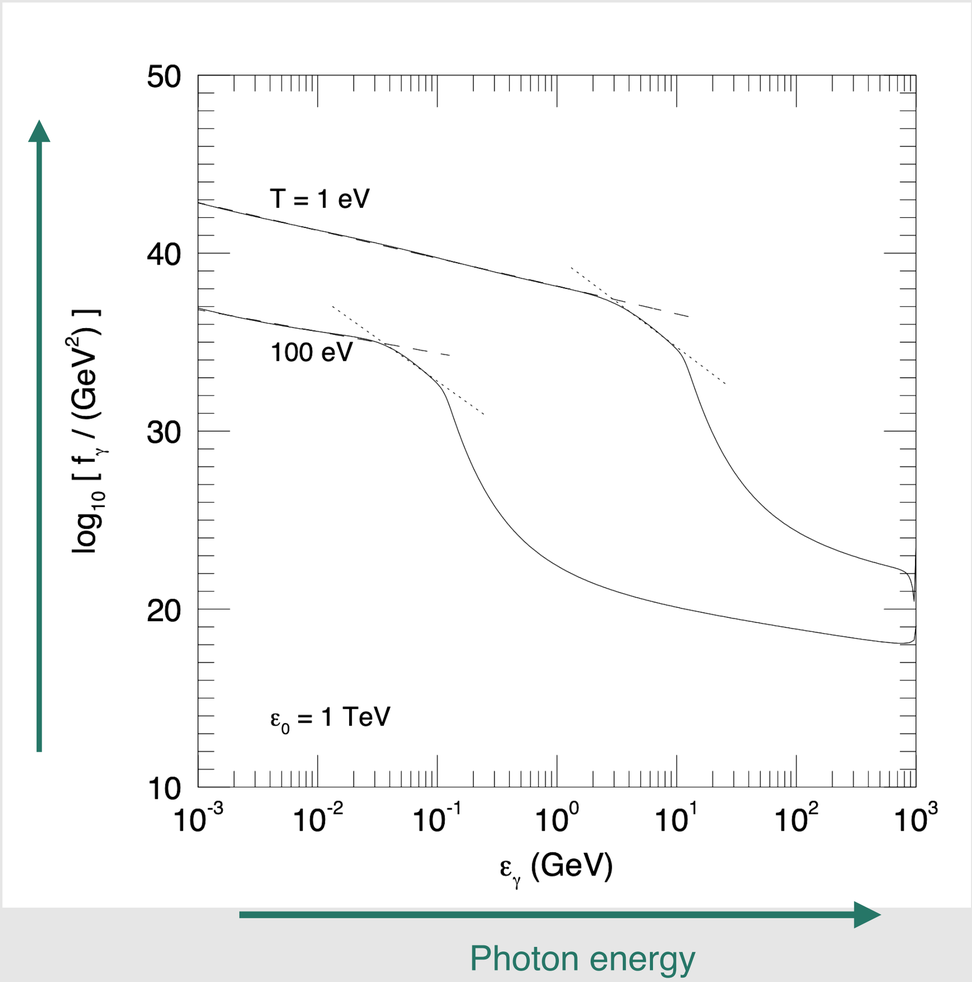
~ # photons

Temperature threshold is

$$E^{\mathrm{th}}_{e^+e^-} \simeq \frac{m_e^2}{22T}$$

At late times, the DM fluid is too diluted for effective annihilations

$T \in [10^{-7}, 10^{-2}]$ MeV : well after standard BBN has ended



from Kawasaki and Moroi (1995) [astro-ph/9412055]

Cascade equations

Solve the cascade equations for $X \in \{\gamma, e^-, e^+\}$

$$f_X(E) = \frac{1}{\Gamma_X(E)}\Big(\underbrace{S_X(E)}_{\text{source term}} + \int_E^\infty dE' \sum_{X'} \underbrace{K_{X'\to X}(E,E') f_{X'}(E')}_{\text{conversion/scattering}} \Big)$$

Cascade equations

Solve the cascade equations for $X \in \{\gamma, e^-, e^+\}$

$$f_X(E) = \frac{1}{\Gamma_X(E)}\Big(\underbrace{S_X(E)}_{\text{source term}} + \int_E^\infty dE' \sum_{X'} \underbrace{K_{X'\to X}(E,E') f_{X'}(E')}_{\text{conversion/scattering}} \Big)$$

Source term contains monochromatic energy injections and final state radiation (FSR) contribution

$$S_X(E) = S_X^{(0)} \delta(E - m_\chi) + S_X^{\text{FSR}}(E)$$

Monochromatic injection depends on the coupling to photons/electrons

$$S_X^{(0)} \propto n_\chi^2 \langle \sigma v \rangle_{\chi\chi \to XX}$$

Final state radiation source accounts for $\chi\chi \to e^+e^-\gamma$ interactions

$$S_\gamma^{\text{FSR}} \propto n_\chi^2 \langle \sigma v \rangle_{\chi\chi \to e^+e^-}$$

Cascade equations

Solve the cascade equations for $X \in \{\gamma, e^-, e^+\}$

$$f_X(E) = \frac{1}{\Gamma_X(E)}\Big(\underbrace{S_X(E)}_{\text{source term}} + \int_E^\infty dE' \sum_{X'} \underbrace{K_{X'\to X}(E,E') f_{X'}(E')}_{\text{conversion/scattering}} \Big)$$

Source term contains monochromatic energy injections and final state radiation (FSR) contribution

$$S_X(E) = S_X^{(0)} \delta(E - m_\chi) + S_X^{\text{FSR}}(E)$$

Monochromatic injection depends on the coupling to photons/electrons

$$S_X^{(0)} \propto n_\chi^2 \langle \sigma v \rangle_{\chi\chi \to XX}$$

Final state radiation source accounts for $\chi\chi \to e^+e^-\gamma$ interactions

$$S_\gamma^{\text{FSR}} \propto n_\chi^2 \langle \sigma v \rangle_{\chi\chi \to e^+e^-}$$

The injected particles scatter via interactions:

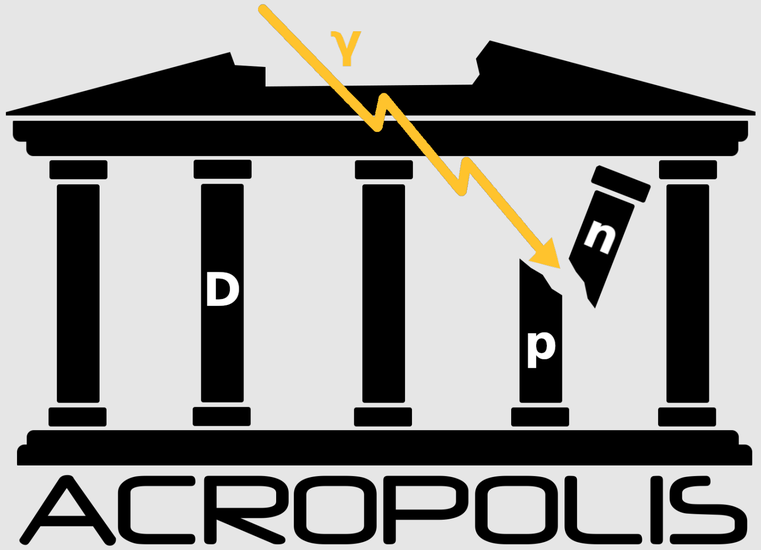
- $\gamma\gamma_{\text{th}} \to e^+e^-$
- $\gamma\gamma_{\text{th}} \to \gamma\gamma$
- $\gamma N \to N e^+e^-$
- $\gamma e^-_{\text{th}} \to \gamma e^-$
- $e^\pm\gamma_{\text{th}} \to e^\pm\gamma$

Tracking the abundances

Light element abundances $N \in \{n, p, \mathrm{D}, {}^3\mathrm{H}, {}^3\mathrm{He}, {}^4\mathrm{He}, {}^7\mathrm{Li}, {}^7\mathrm{Be}\}$ are tracked via

$$\frac{dT}{dt}\frac{dY_N}{dT} = \sum_{N_i} \underbrace{Y_{N_i} \int_0^\infty dE f_\gamma(E) \sigma_{\gamma + N_i \to N}(E)}_{\text{creation}} - \underbrace{Y_N \sum_{N_f} \int_0^\infty dE f_\gamma(E) \sigma_{\gamma + N \to N_f}(E)}_{\text{destruction}}$$

No.		E^{th} [MeV]
1	$\mathrm{D} + \gamma \to p + n$	2.22
2	${}^3\mathrm{H} + \gamma \to \mathrm{D} + n$	6.26
3	${}^3\mathrm{H} + \gamma \to p + n + n$	8.48
4	${}^3\mathrm{He} + \gamma \to \mathrm{D} + p$	5.49
5	${}^3\mathrm{He} + \gamma \to n + p + p$	7.12
6	${}^4\mathrm{He} + \gamma \to {}^3\mathrm{H} + p$	19.81
7	${}^4\mathrm{He} + \gamma \to {}^3\mathrm{He} + n$	20.58
8	${}^4\mathrm{He} + \gamma \to \mathrm{D} + \mathrm{D}$	23.84
9	${}^4\mathrm{He} + \gamma \to \mathrm{D} + n + p$	26.07



In principle complicated system —> ACROPOLIS

Depta, Hufnagel, Schmidt-Hoberg (2021)

Why resonant annihilations?

Why resonant annihilations?

Consider dark sector with resonance

$$m_R \equiv m_\chi(2 + \delta_R), \quad \delta_R \ll 1$$

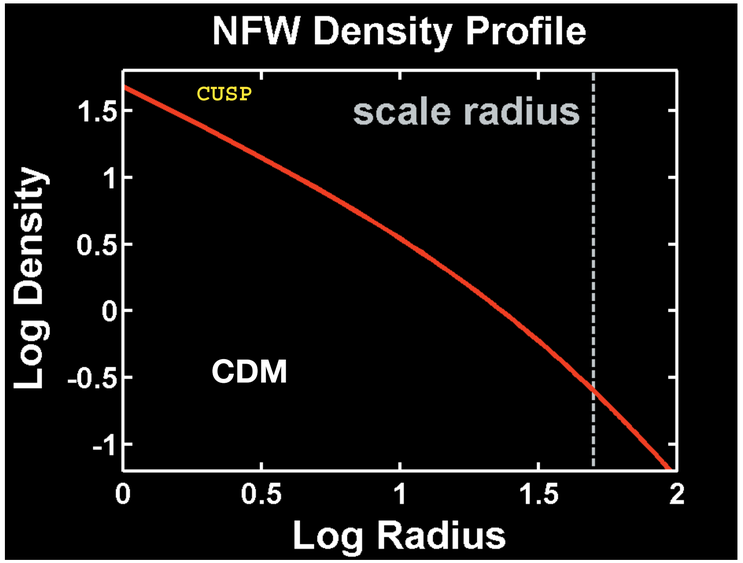
Intermezzo: core vs cusp

DM density profiles: how the DM is distributed in a (galaxy/cluster) halo

Self-interactions alter the DM halo shape

Collisionless dark matter (CDM) predicts cuspy Navarro-Frenk-White profile

$$\rho(r)^{\mathrm{NFW}} \propto (r/r_s)^{-1}(1+r/r_s)^{-2}$$



Del Popolo et al. [2209.14151]

Intermezzo: core vs cusp

DM density profiles: how the DM is distributed in a (galaxy/cluster) halo

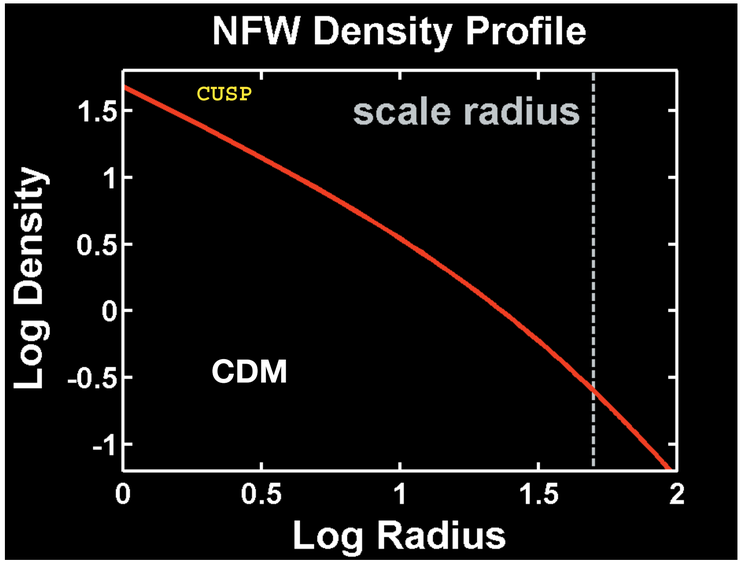
Self-interactions alter the DM halo shape

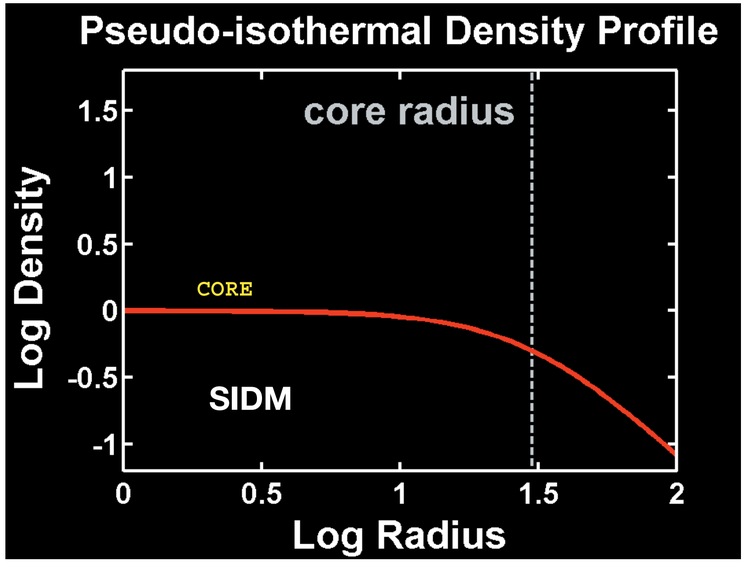
Collisionless dark matter (CDM) predicts cuspy Navarro-Frenk-White profile

$$\rho(r)^{\mathrm{NFW}} \propto (r/r_s)^{-1}(1+r/r_s)^{-2}$$

Self-interacting DM (SIDM) predicts core-like profile: NFW at large r, in center efficient heat transfer (isothermal)

$$\rho(r)^{\mathrm{SIDM}} \propto \begin{cases} \text{const.} & r \ll r_1 \\ \rho(r)^{\mathrm{NFW}} & r \gg r_1 \end{cases}$$





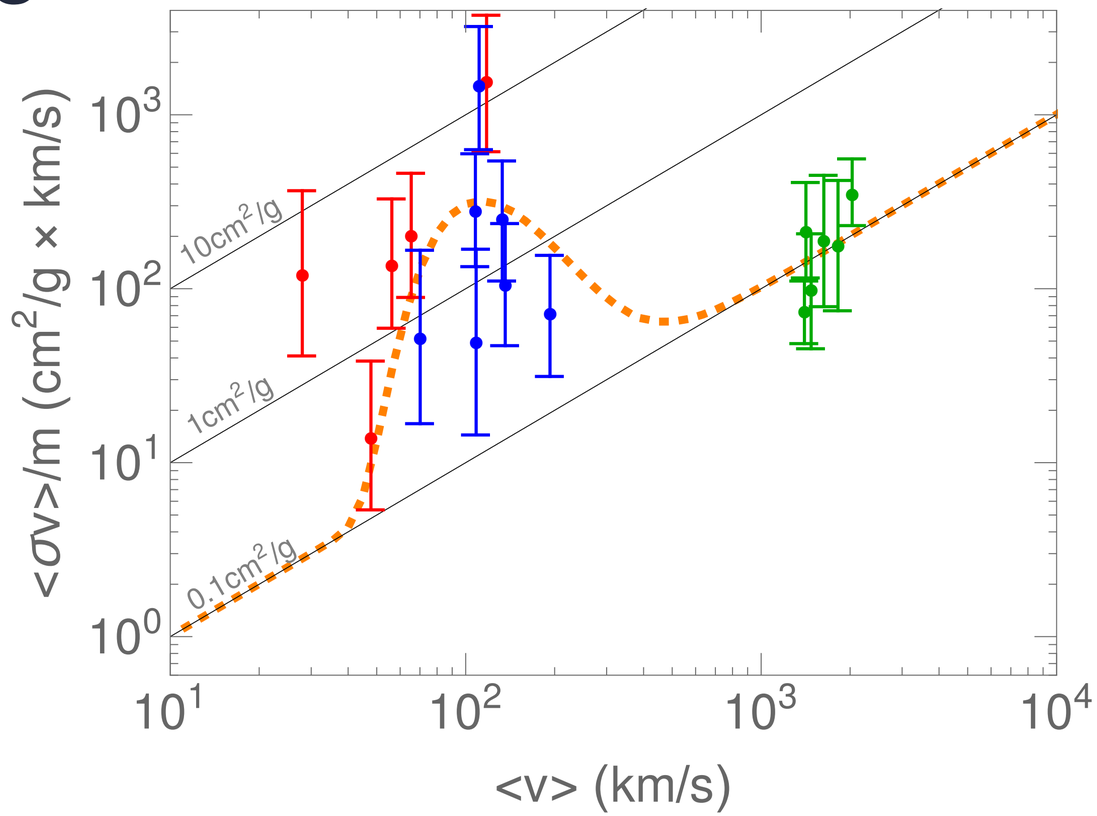
Del Popolo et al. [2209.14151]

Intermezzo: resonant self-scattering

Observations hint* at SIDM density profiles with self-interaction strengths

$$\frac{\sigma}{m} \sim 0.1 - 1 \ \mathrm{cm}^2/\mathrm{g}$$

and velocity dependence to accommodate observations at different scales



Adapted from Chu et al. [1810.04709]

*jury's still out on this one

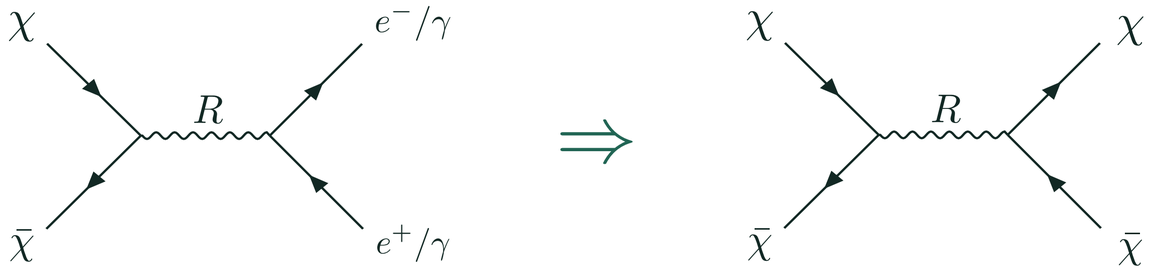
Intermezzo: resonant self-scattering

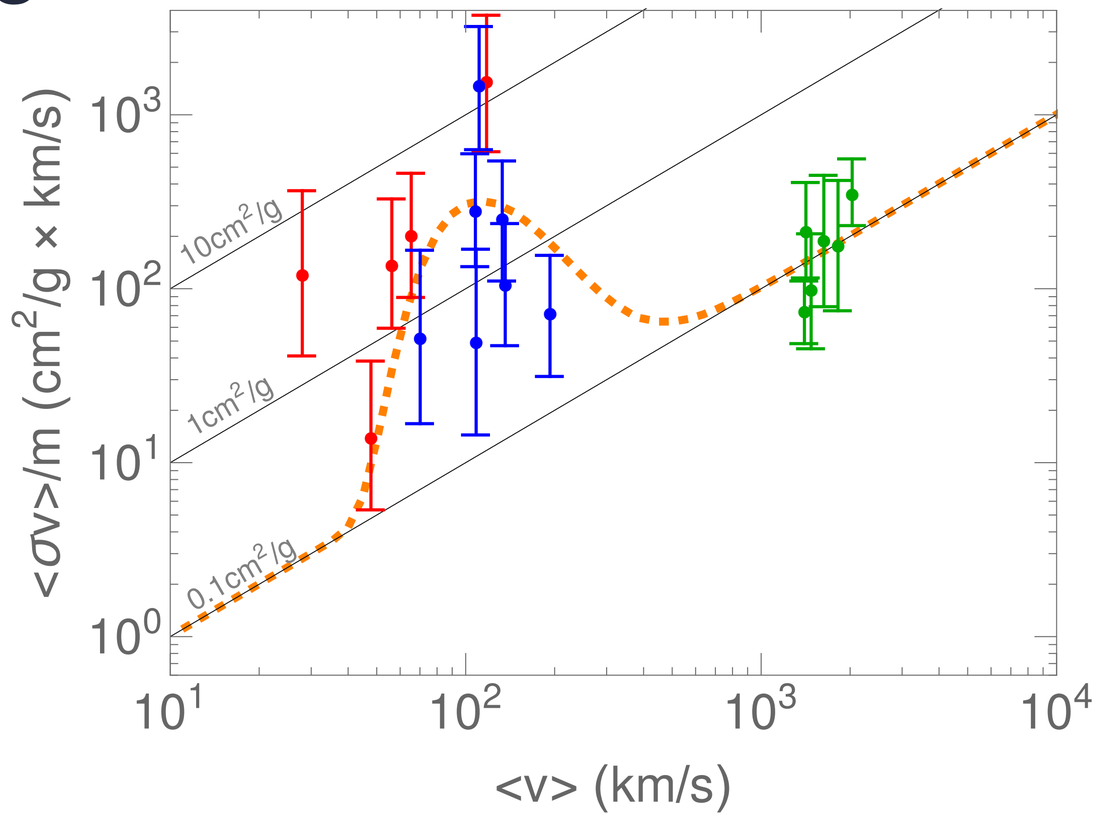
Observations hint* at SIDM density profiles with self-interaction strengths

$$\frac{\sigma}{m} \sim 0.1 - 1 \text{ cm}^2/\text{g}$$

and velocity dependence to accommodate observations at different scales

For any electrophilic model, we also expect (sizeable) self-interactions





Adapted from Chu et al. [1810.04709]

*jury's still out on this one

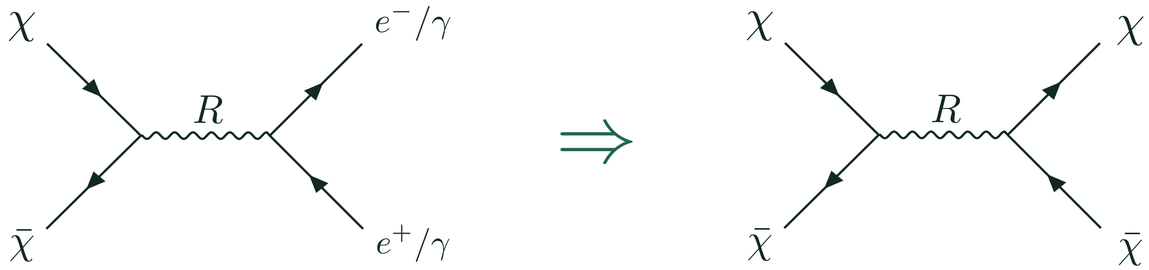
Intermezzo: resonant self-scattering

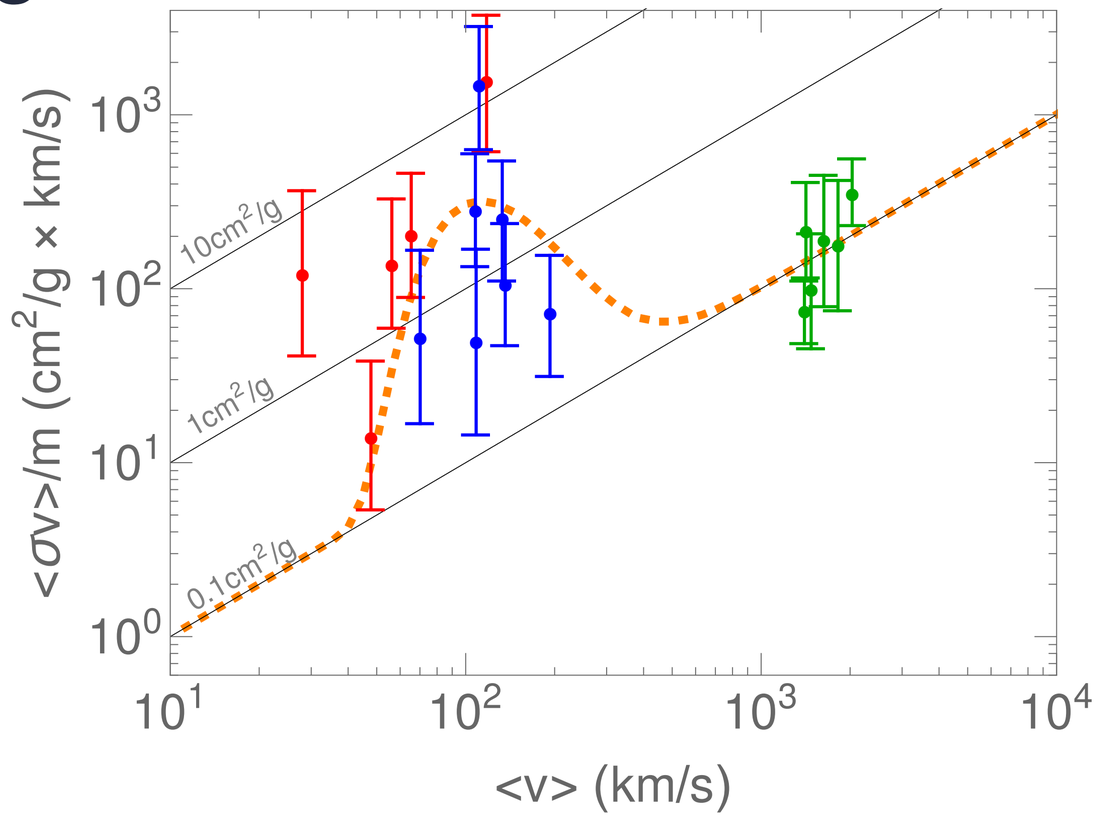
Observations hint* at SIDM density profiles with self-interaction strengths

$$\frac{\sigma}{m} \sim 0.1 - 1 \text{ cm}^2/\text{g}$$

and velocity dependence to accommodate observations at different scales

For any electrophilic model, we also expect (sizeable) self-interactions





Adapted from Chu et al. [1810.04709]

Typical velocity peaks at galaxy halo sizes, which dictates resonance mass

$$v_R \equiv 2\sqrt{\delta_R} \sim 10^2 \,\text{km/s} \quad \Rightarrow \quad \delta_R \sim 10^{-8}$$

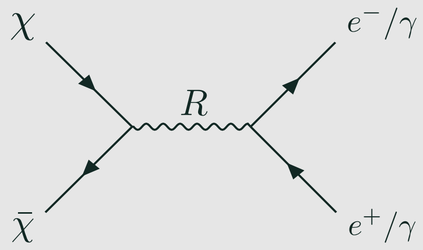
*jury's still out on this one

Why resonant annihilations?

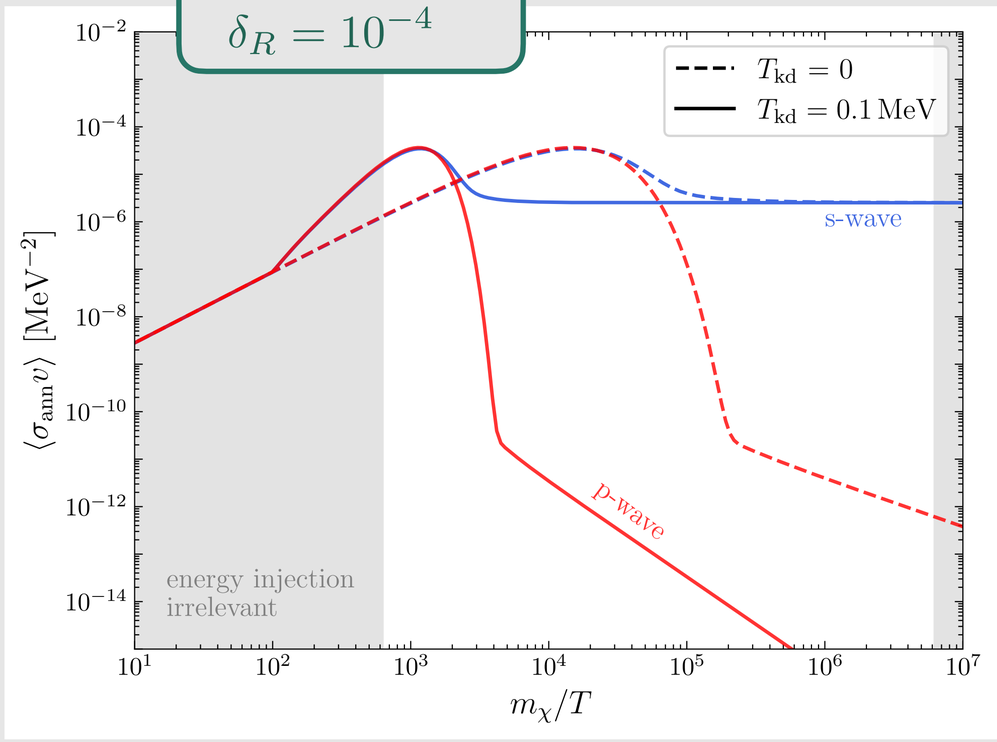
Consider dark sector with resonance

$$m_R \equiv m_\chi(2+\delta_R), \quad \delta_R \ll 1$$

For MeV scale DM, annihilations peak in photodisintegration window!



Injected power



Time

Why resonant annihilations?

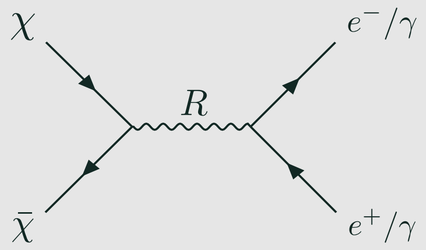
Consider dark sector with resonance

$$m_R \equiv m_\chi(2+\delta_R), \quad \delta_R \ll 1$$

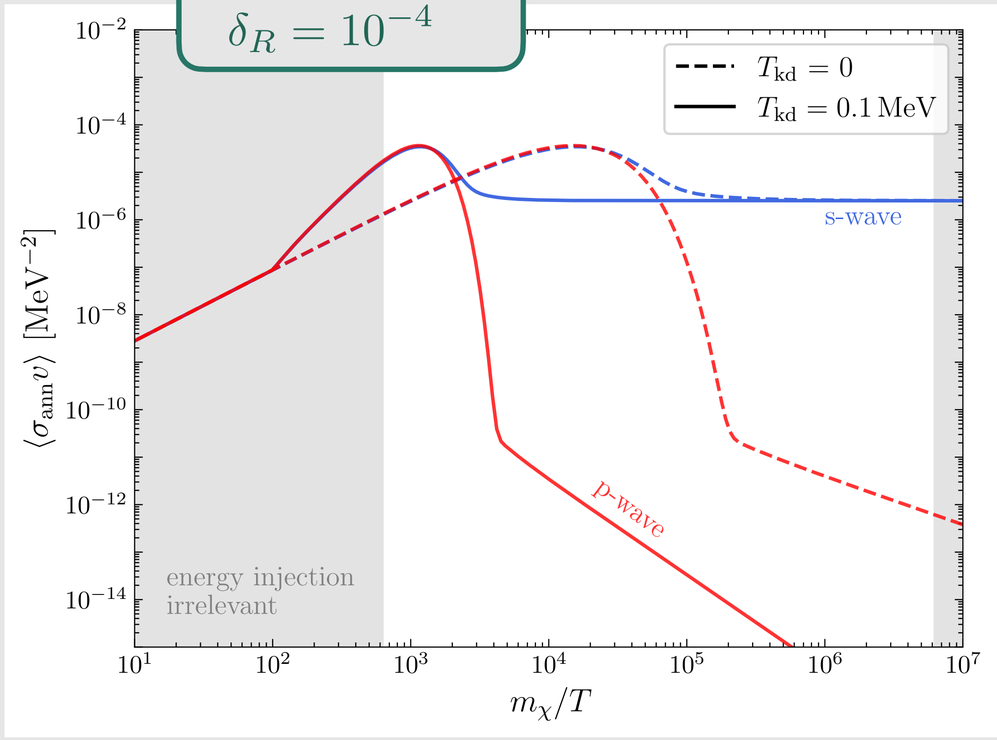
For MeV scale DM, annihilations peak in photodisintegration window!

We can write the annihilation cross section as

$$\sigma_{\rm ann}^{\rm res} = \frac{4\pi S}{m_\chi E(v)} \frac{\Gamma_d(v)\Gamma_v(v_f)/4}{(E(v)-E(v_R))^2+\Gamma(v)^2/4}, \quad v_R \equiv 2\sqrt{\delta_R}$$



Injected power



Time

Why resonant annihilations?

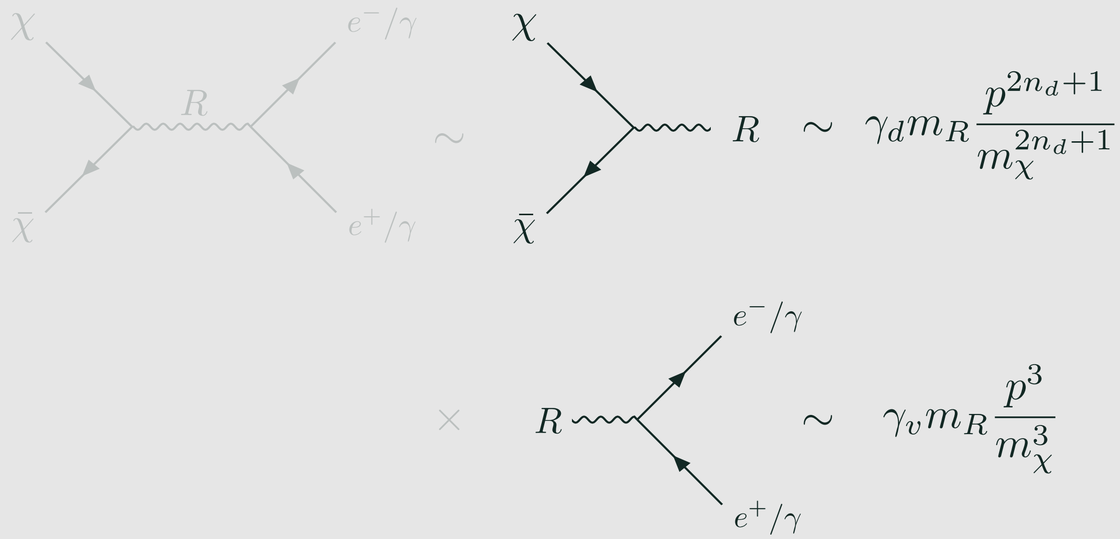
Consider dark sector with resonance

$$m_R \equiv m_\chi(2+\delta_R), \quad \delta_R \ll 1$$

For MeV scale DM, annihilations peak in photodisintegration window!

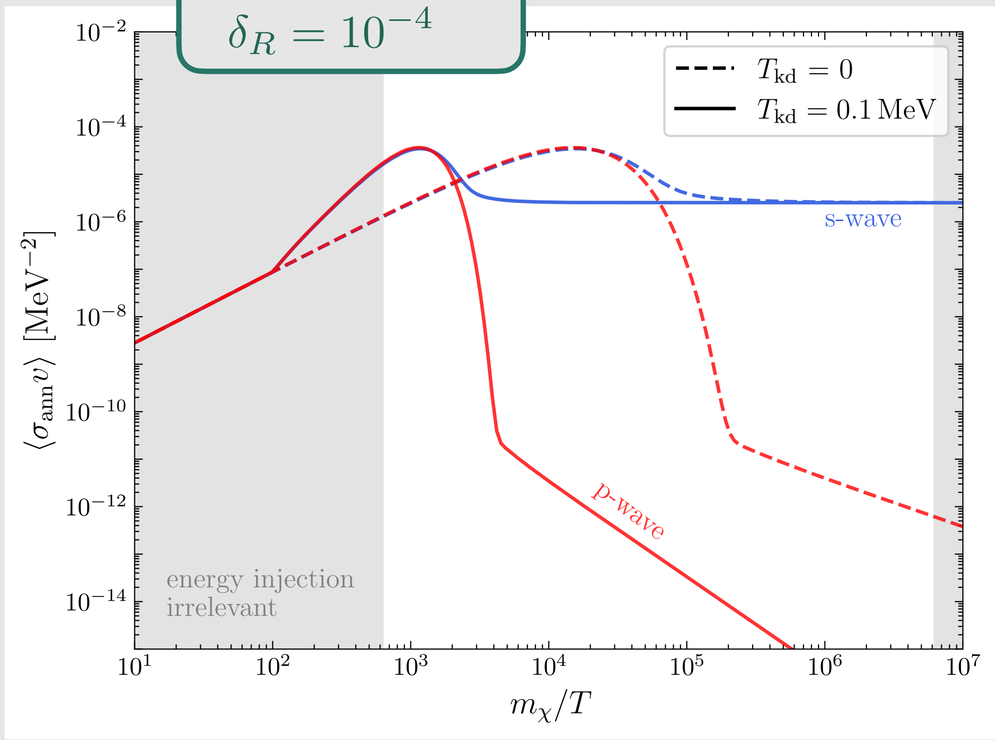
We can write the annihilation cross section as

$$\sigma_{\rm ann}^{\rm res} = \frac{4\pi S}{m_\chi E(v)} \frac{\Gamma_d(v)\Gamma_v(v_f)/4}{(E(v)-E(v_R))^2+\Gamma(v)^2/4}, \quad v_R \equiv 2\sqrt{\delta_R}$$



$m_\chi = 10\,\text{MeV}$

$\delta_R = 10^{-4}$



γ_d : dark coupling

γ_v : visible coupling

$n_d = 0$ $s-$wave

$n_d = 1$ $p-$wave

Model independent setup!

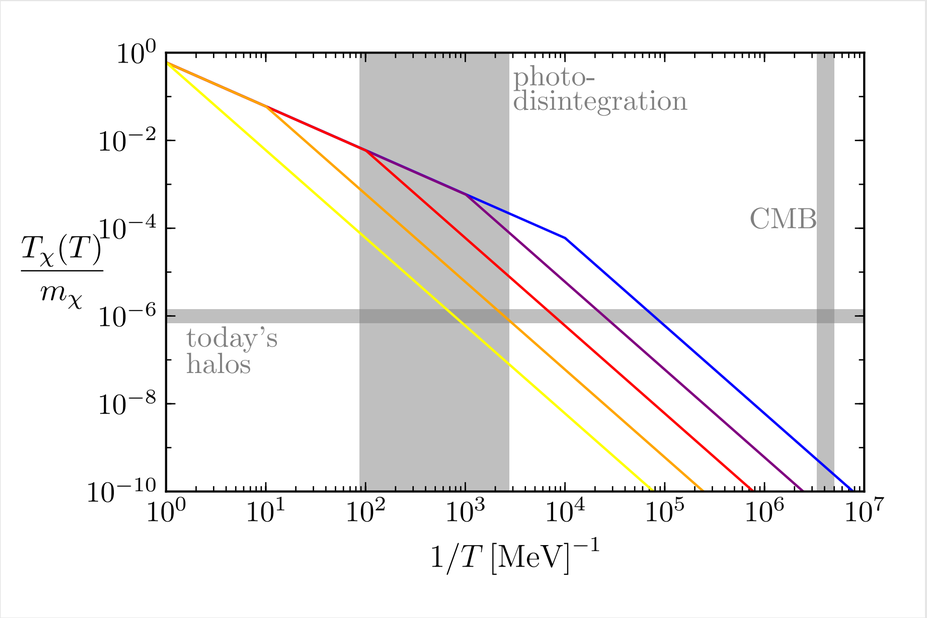
Temperature dependence

Injected energy depends on the thermally averaged cross section

$$\langle \sigma v \rangle_{\rm ann} \overset{T_\chi \ll m_\chi}{=} \frac{4 T_\chi^{3/2}}{\sqrt{\pi} m_\chi^{11/2}} \int_0^\infty \mathrm{d}p^2 e^{-p^2 T_\chi / m_\chi^3} p^2 \sigma$$

with DM temperature

$$T_\chi(T) = \begin{cases} T & \text{for} \quad T \geq T_{\rm kd} \\ T_{\rm kd} R(T_{\rm kd})^2 / R(T)^2 & \text{for} \quad T < T_{\rm kd} \end{cases}$$



Adapted from Depta et al. (2019) [arXiv.1901.06944]

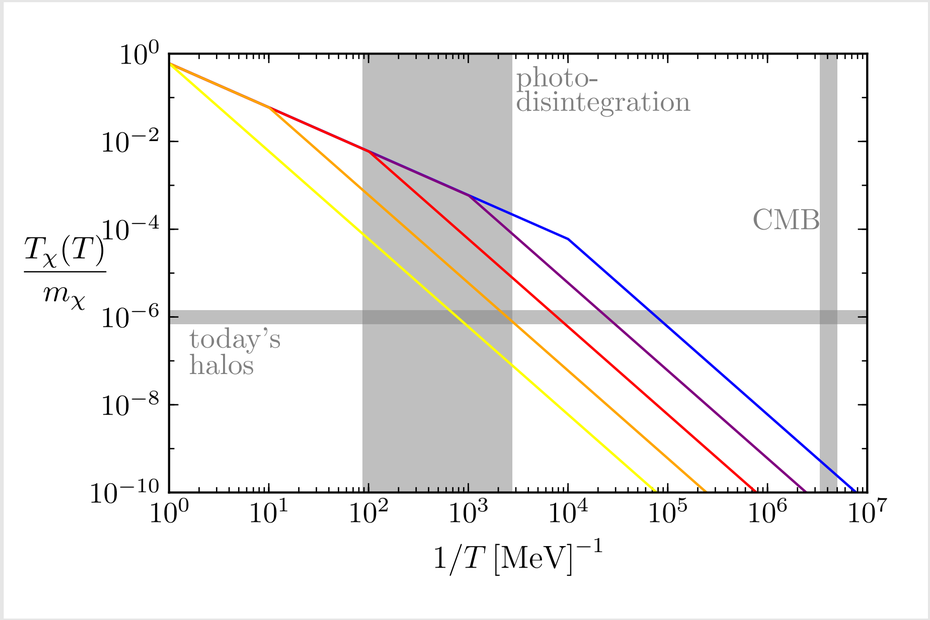
Temperature dependence

Injected energy depends on the thermally averaged cross section

$$\langle \sigma v \rangle_{\rm ann} \overset{T_\chi \ll m_\chi}{=} \frac{4 T_\chi^{3/2}}{\sqrt{\pi} m_\chi^{11/2}} \int_0^\infty {\rm d}p^2 e^{-p^2 T_\chi / m_\chi^3} p^2 \sigma$$

with DM temperature

$$T_\chi(T) = \begin{cases} T & \text{for} \quad T \geq T_{\rm kd} \\ T_{\rm kd} R(T_{\rm kd})^2 / R(T)^2 & \text{for} \quad T < T_{\rm kd} \end{cases}$$



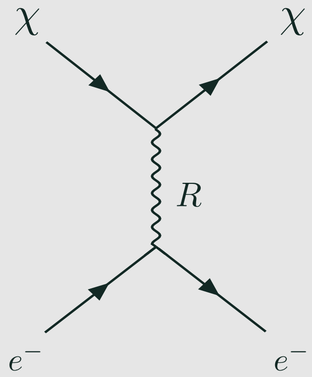
Adapted from Depta et al. (2019) [arXiv.1901.06944]

Kinetic decoupling when scattering becomes inefficient, i.e. when

$$\Gamma = n_e \langle \sigma v \rangle_{\chi e \to \chi e} \big|_{T = T_{\rm kd}} \lesssim H(T_{\rm kd})$$

Scattering is related to annihilation via crossing symmetry

$$\sigma_{\chi e^- \to \chi e^-} = C \gamma_v \gamma_d \frac{p^2}{m_\chi^4}, \quad C = \mathcal{O}(1) \qquad T \gtrsim m_e$$



Temperature dependence

Injected energy depends on the thermally averaged cross section

$$\langle \sigma v \rangle_{\rm ann} \overset{T_\chi \ll m_\chi}{=} \frac{4 T_\chi^{3/2}}{\sqrt{\pi} m_\chi^{11/2}} \int_0^\infty {\rm d}p^2 e^{-p^2 T_\chi / m_\chi^3} p^2 \sigma$$

with DM temperature

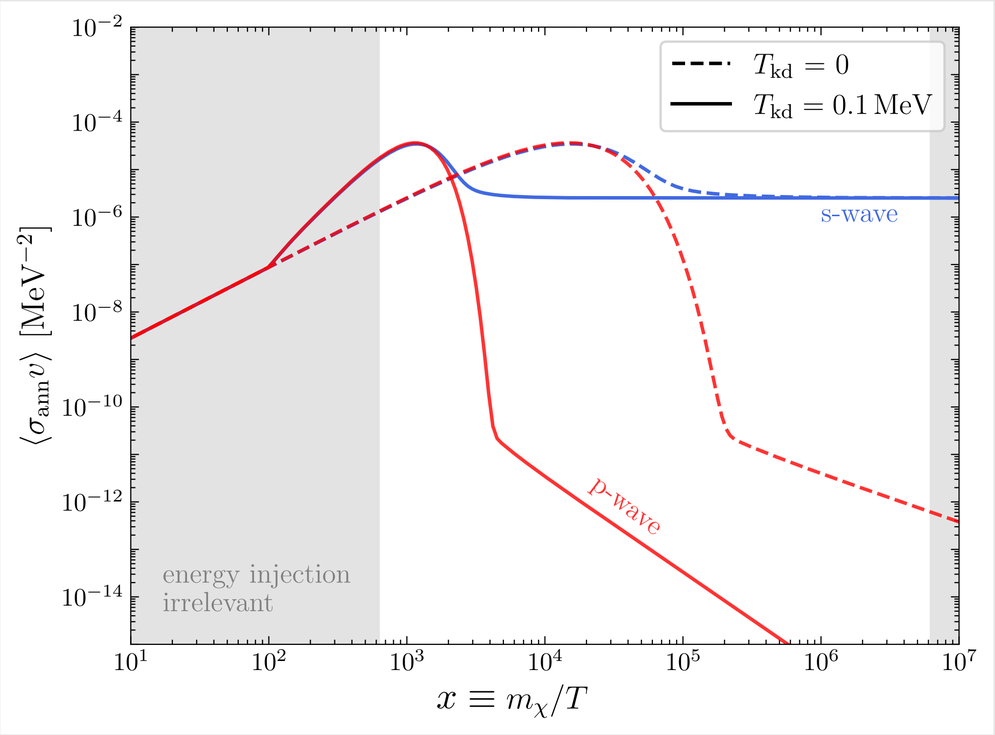
$$T_\chi(T) = \begin{cases} T & \text{for} \quad T \geq T_{\rm kd} \\ T_{\rm kd} R(T_{\rm kd})^2 / R(T)^2 & \text{for} \quad T < T_{\rm kd} \end{cases}$$

Kinetic decoupling when scattering becomes inefficient, i.e. when

$$\Gamma = n_e \langle \sigma v \rangle_{\chi e \to \chi e} \big|_{T = T_{\rm kd}} \lesssim H(T_{\rm kd})$$

Scattering is related to annihilation via crossing symmetry

$$\sigma_{\chi e^- \to \chi e^-} = C \gamma_v \gamma_d \frac{p^2}{m_\chi^4}, \quad C = \mathcal{O}(1) \qquad T \gtrsim m_e$$



The resonance and off-resonance contributions are

$$\langle \sigma_{\rm ann} v \rangle^{\rm res} \propto \gamma_v \frac{x^{3/2}}{m_\chi^2} e^{-\delta_R x}, \quad (\gamma_v \ll \gamma_d)$$

$$\langle \sigma_{\rm ann} v \rangle^{\text{off-res}} \propto \frac{\gamma_v \gamma_d}{m_\chi^2 \delta_R^2} x^{-n_d}$$

Implementation in ACROPOLIS

Updated version of ACROPOLIS

As of v.1.2.3, ACROPOLIS can handle two physical models;

- `DecayModel`: for decaying DM models

$$\phi \to e^+e^-/\gamma\gamma$$

- `AnnihilationModel`: for DM annihilations

$$\chi\bar{\chi} \to e^+e^-/\gamma\gamma$$

The updated v.1.3.0 introduces the new `ResonanceModel`: annihilations via resonant state

$$\chi\bar{\chi} \to R \to e^+e^-$$

Updated version of ACROPOLIS

As of v.1.2.3, ACROPOLIS can handle two physical models;

- `DecayModel`: for decaying DM models

$$\phi \to e^+e^-/\gamma\gamma$$

- `AnnihilationModel`: for DM annihilations

$$\chi\bar{\chi} \to e^+e^-/\gamma\gamma$$

The updated v.1.3.0 introduces the new `ResonanceModel`: annihilations via resonant state

$$\chi\bar{\chi} \to R \to e^+e^-$$

Initialize the model:

```
# ext.models
from acropolis.ext.models import ResonanceModel

# Initalize the model
model = ResonanceModel(
    mchi    = 10.  , ..... m_χ
    delta   = 1e-2, ..... δ_R
    gammad  = 1e-5, ..... γ_d
    gammav  = 1e-3, ..... γ_v
    nd      = 0    , ..... n_d
    tempkd  = 1e-2  ..... T_kd
)
```

Updated version of ACROPOLIS

As of v.1.2.3, ACROPOLIS can handle two physical models;

- `DecayModel`: for decaying DM models

$$\phi \to e^+e^-/\gamma\gamma$$

- `AnnihilationModel`: for DM annihilations

$$\chi\bar{\chi} \to e^+e^-/\gamma\gamma$$

The updated v.1.3.0 introduces the new `ResonanceModel`: annihilations via resonant state

$$\chi\bar{\chi} \to R \to e^+e^-$$

Initialize the model:

```
# ext.models
from acropolis.ext.models import ResonanceModel

# Initalize the model
model = ResonanceModel(
      mchi    = 10.  ,  # m_χ
      delta   = 1e-2,   # δ_R
      gammad  = 1e-5,   # γ_d
      gammav  = 1e-3,   # γ_v
      nd      = 0    ,  # n_d
      tempkd  = 1e-2    # T_kd
)
```

And run the code

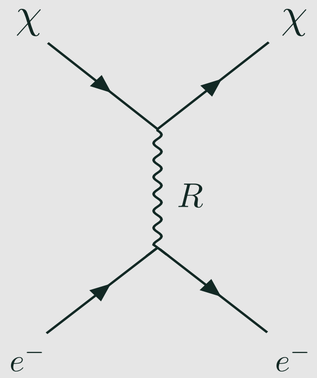
```
# Run photodisintegration
Yf = model.run_disintegration()
```

Output will be the altered light element abundances with theoretical uncertainties

Benchmark models and parameter space scans

Code works for any model that features a resonant state, but we provide three benchmark models

model	χ	R	Lagrangian	n_d	γ_d	γ_v
2 Scalars $(\varphi + \Phi)$	φ	Φ	$g_1\varphi\varphi\Phi + g_2\bar{e}e\Phi$	0	$\frac{g_1^2}{64\pi m_\varphi^2}$	$\frac{g_2^2}{8\pi}$
Fermion (ψ) + Vector (A'_μ)	ψ	A'_μ	$g_1\bar{\psi}\gamma^\mu\psi A'_\mu + g_2\bar{e}\gamma^\mu e A'_\mu$	0	$\frac{g_1^2}{8\pi}$	$\frac{g_2^2}{12\pi}$
Scalar (φ) + Vector (A'_μ)	φ	A'_μ	$g_1\varphi^\dagger \overleftrightarrow{\partial}_\mu \varphi A'^\mu + g_2\bar{e}\gamma^\mu e A'_\mu$	1	$\frac{g_1^2}{48\pi}$	$\frac{g_2^2}{12\pi}$

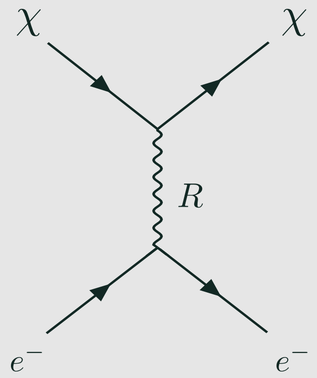


Allows dynamical determination of the decoupling temperature

Benchmark models and parameter space scans

Code works for any model that features a resonant state, but we provide three benchmark models

model	χ	R	Lagrangian	n_d	γ_d	γ_v
2 Scalars ($\varphi + \Phi$)	φ	Φ	$g_1\varphi\varphi\Phi + g_2\bar{e}e\Phi$	0	$\frac{g_1^2}{64\pi m_\varphi^2}$	$\frac{g_2^2}{8\pi}$
Fermion (ψ) + Vector (A'_μ)	ψ	A'_μ	$g_1\bar{\psi}\gamma^\mu\psi A'_\mu + g_2\bar{e}\gamma^\mu e A'_\mu$	0	$\frac{g_1^2}{8\pi}$	$\frac{g_2^2}{12\pi}$
Scalar (φ) + Vector (A'_μ)	φ	A'_μ	$g_1\varphi^\dagger \overleftrightarrow{\partial}_\mu \varphi A'^\mu + g_2\bar{e}\gamma^\mu e A'_\mu$	1	$\frac{g_1^2}{48\pi}$	$\frac{g_2^2}{12\pi}$



Allows dynamical determination of the decoupling temperature

Running a parameter space scan for BM model 3 for $N \times N$ points in the $m_\chi - \gamma_v$ plane

```
# scans
from acropolis.scans import BufferedScanner, ScanParameter
# ext.benchmarks
from acropolis.ext.benchmarks import BenchmarkModel3

scan_result = BufferedScanner( BenchmarkModel3,
                               mchi   = ScanParameter(0, 3, N),
                               delta  = 1e-2,
                               gammad = 1e-3,
                               gammav = ScanParameter(-14, -2, N),
                             ).perform_scan(cores=-1)
```

Results

What happens to the abundances?

Non-resonant annihilations

$$\langle \sigma_{\rm ann} v \rangle \simeq a + b \langle v_{\rm rel}^2 \rangle, \qquad \langle v_{\rm rel}^2 \rangle \simeq \frac{6 T_\chi}{m_\chi}$$

Away from the resonance, the annihilation strength is

$$\langle \sigma_{\rm ann} v \rangle^{\text{off-res}} \simeq \frac{16 S \sqrt{\pi} \gamma_d \gamma_v}{m_\chi^2 \delta_R^2} x^{-n_d} \bar{\Gamma}(n_d + 3/2),$$

$$a = \frac{8\pi \gamma_d \gamma_v}{m_\chi^2 \delta_R^2}$$

$$b = \frac{2\pi \gamma_d \gamma_v}{m_\chi^2 \delta_R^2}$$

What happens to the abundances?

Non-resonant annihilations

$$\langle \sigma_{\rm ann} v \rangle \simeq a + b \langle v_{\rm rel}^2 \rangle, \quad \langle v_{\rm rel}^2 \rangle \simeq \frac{6 T_\chi}{m_\chi}$$

Away from the resonance, the annihilation strength is

$$\langle \sigma_{\rm ann} v \rangle^{\text{off-res}} \simeq \frac{16 S \sqrt{\pi} \gamma_d \gamma_v}{m_\chi^2 \delta_R^2} x^{-n_d} \bar{\Gamma}(n_d + 3/2),$$

$$a = \frac{8\pi \gamma_d \gamma_v}{m_\chi^2 \delta_R^2}$$

$$b = \frac{2\pi \gamma_d \gamma_v}{m_\chi^2 \delta_R^2}$$

Use BBN observations

$$\mathcal{Y}_p = 0.245 \pm 0.003,$$

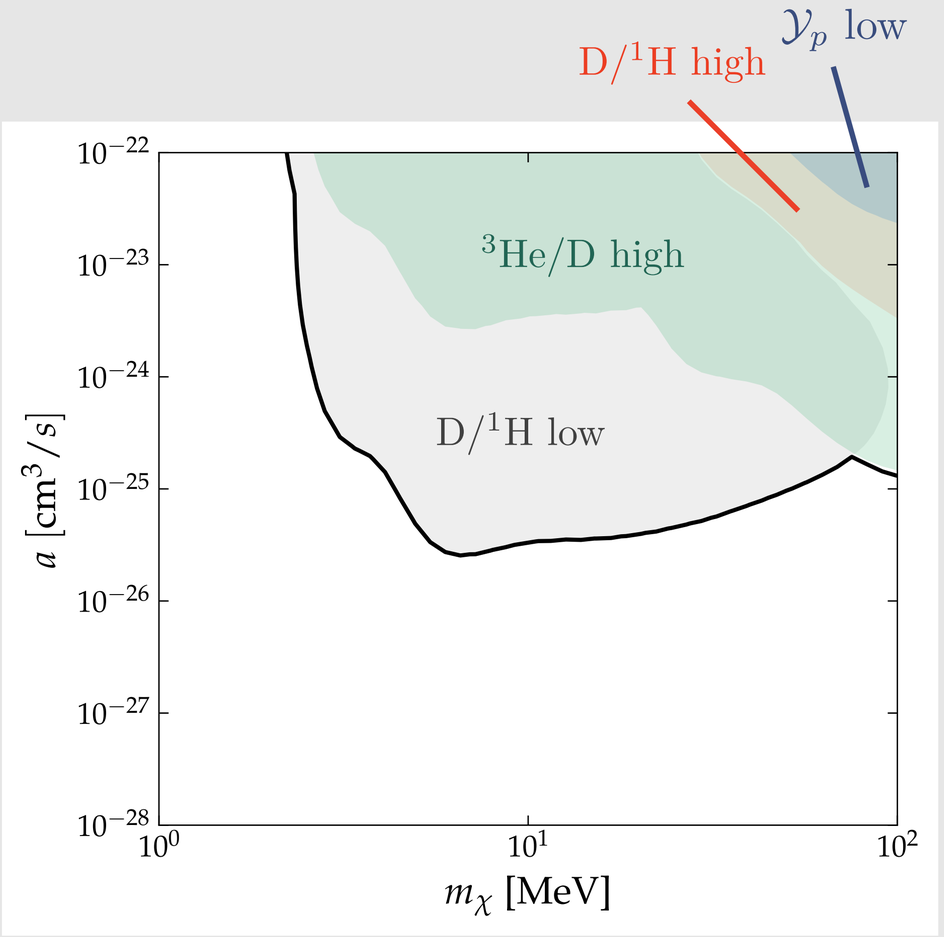
PDG (2022)

$$\mathrm{D}/^1\mathrm{H} = (25.47 \pm 0.25) \times 10^{-6}$$

$$^3\mathrm{He}/\mathrm{D} = (8.3 \pm 1.5) \times 10^{-1}$$

Geiss and Gloecker (2003)

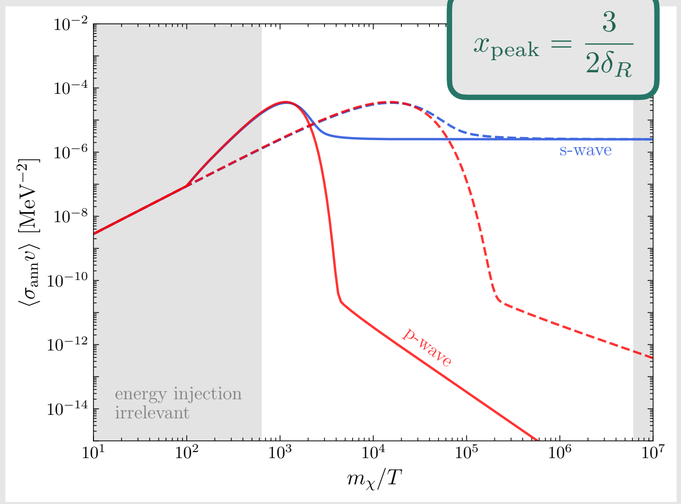
Deuterium abundance is most sensitive to the photodisintegration

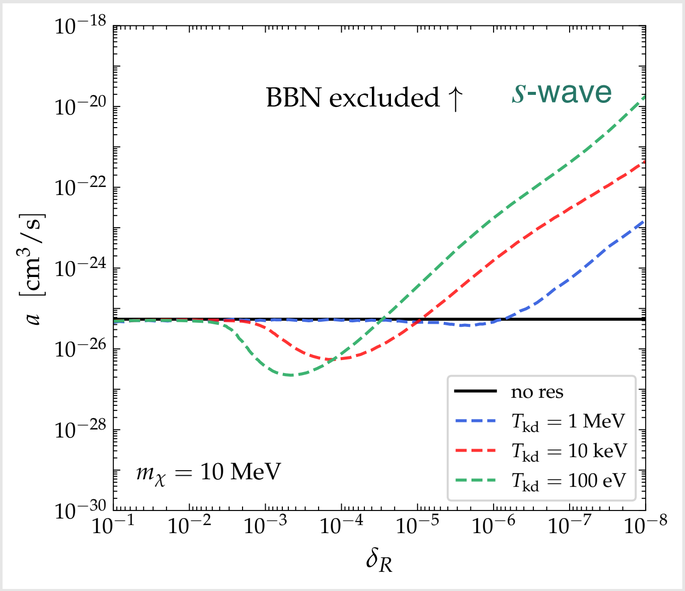


δ_R dependence

Can identify three regions;

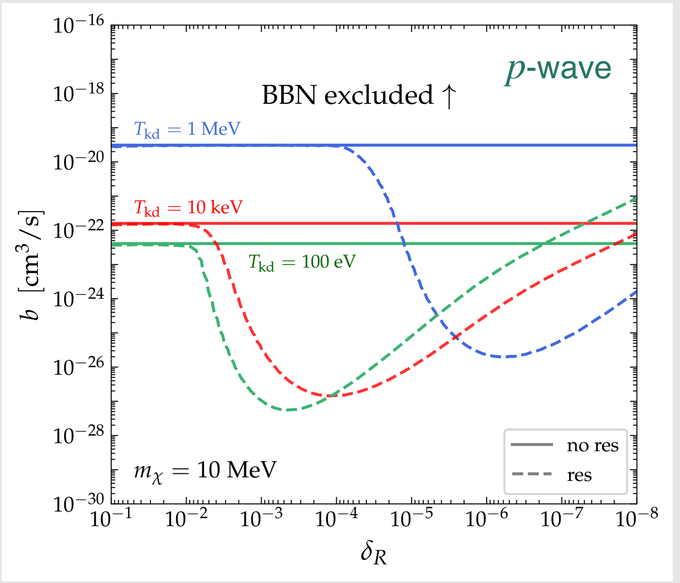
- Large δ_R: resonance peaks too early
- Intermediate δ_R: strong resonance peak
- Small δ_R: the resonance bounds are weaker than the non-resonant case





Overall;

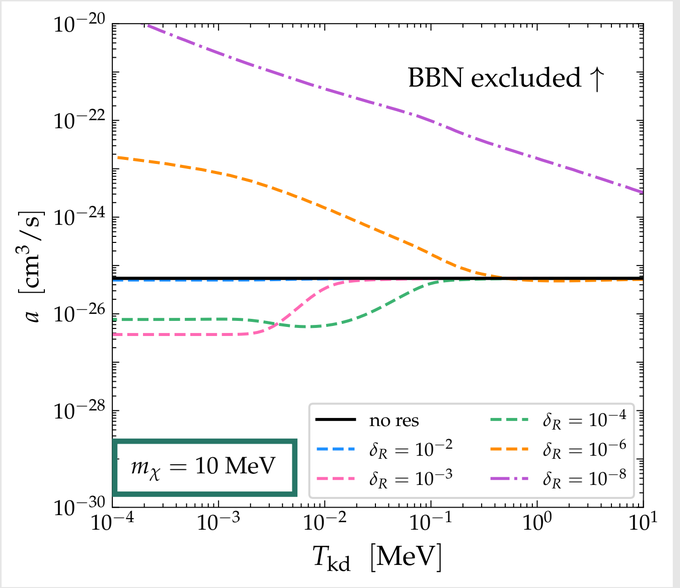
- the p-wave resonances are stronger
- strong $T_{\rm kd}$ dependence

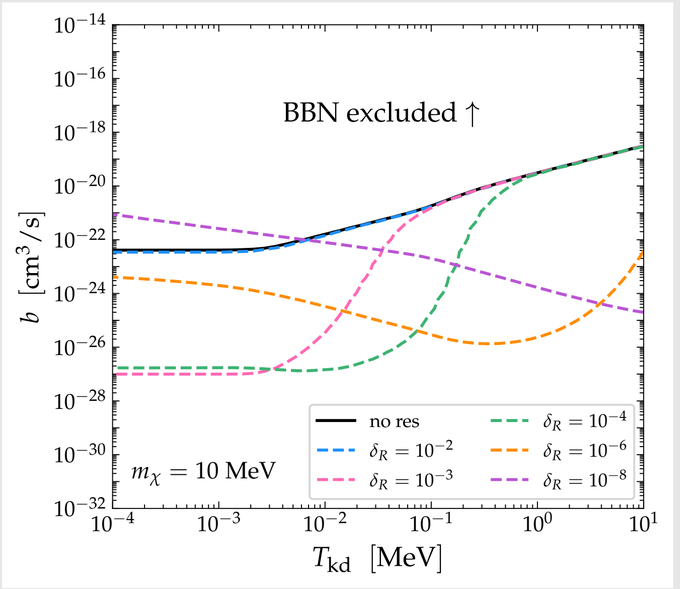


T_{kd} dependence

Low masses: early decoupling suppresses resonance effect

If decoupling happens significantly late, resonance model suffers from stronger bounds

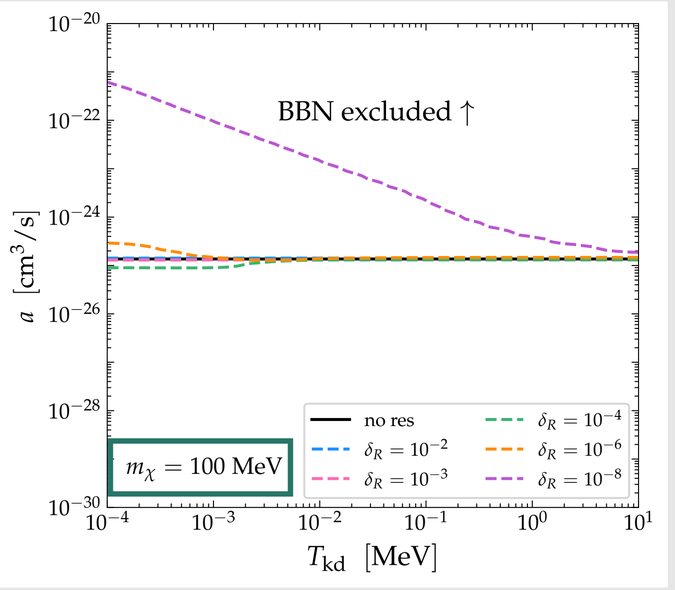




$T_{\rm kd}$ dependence

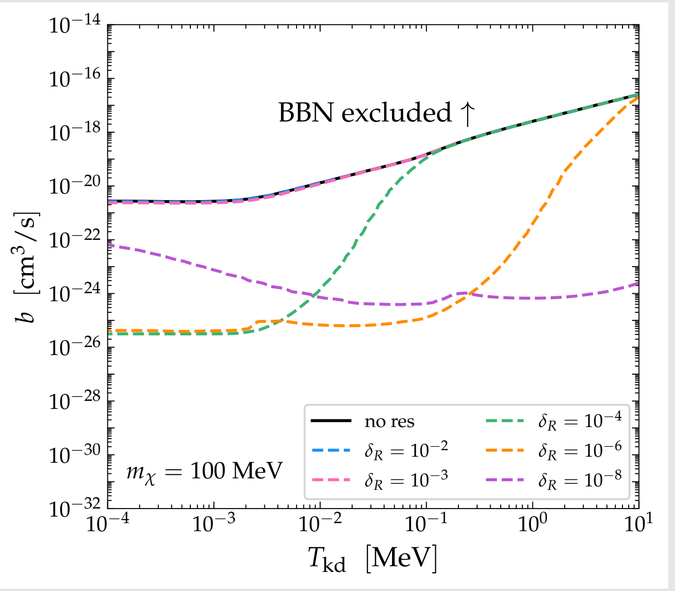
Low masses: early decoupling suppresses resonance effect

If decoupling happens significantly late, resonance model suffers from stronger bounds



Larger masses: s-wave resonance barely noticeable

For p-wave, the narrow resonances are strongly constrained

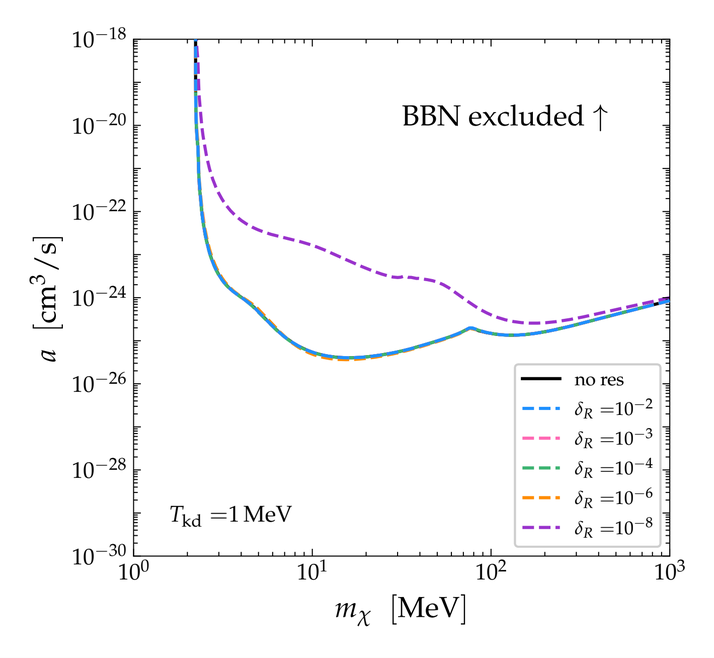


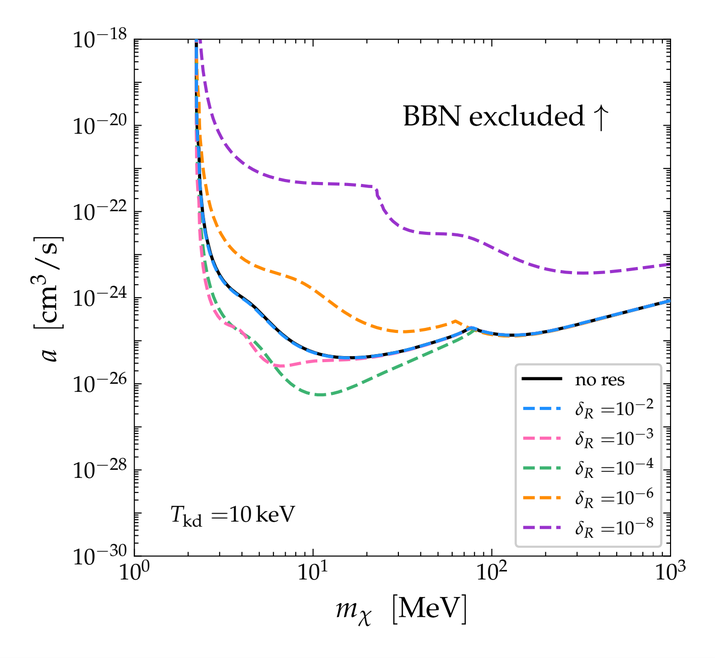
Across the board: larger masses are typically less constrained

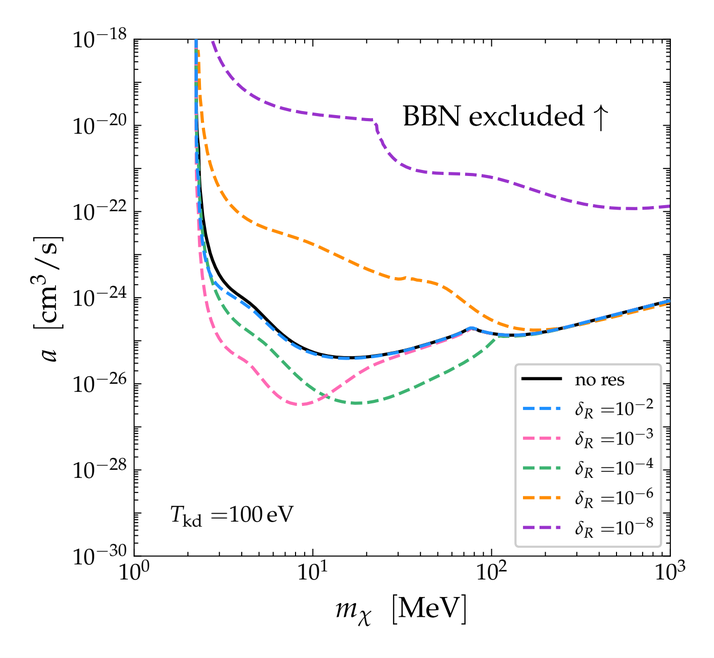
Results (s-wave), fixed $T_{\rm kd}$

$$a = \frac{8\pi\gamma_d\gamma_v}{m_\chi^2\delta_R^2}$$

Fixed $T_{\rm kd}$: resonance effect is observable if the decoupling temperature is low enough







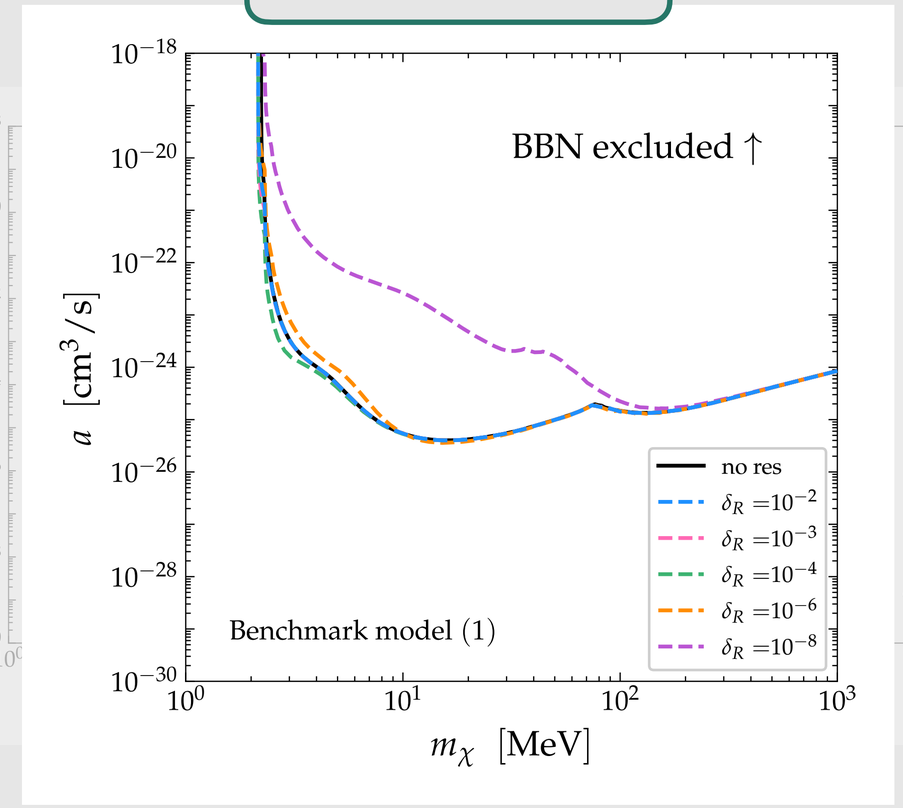
Results (s-wave), dynamical $T_{\rm kd}$

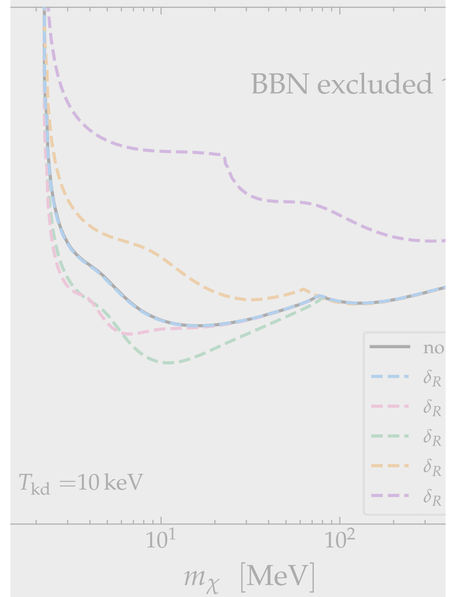
$$a = \frac{8\pi\gamma_d\gamma_v}{m_\chi^2\delta_R^2}$$

Fixed $T_{\rm kd}$: resonance effect is observable if the decoupling temperature is low enough

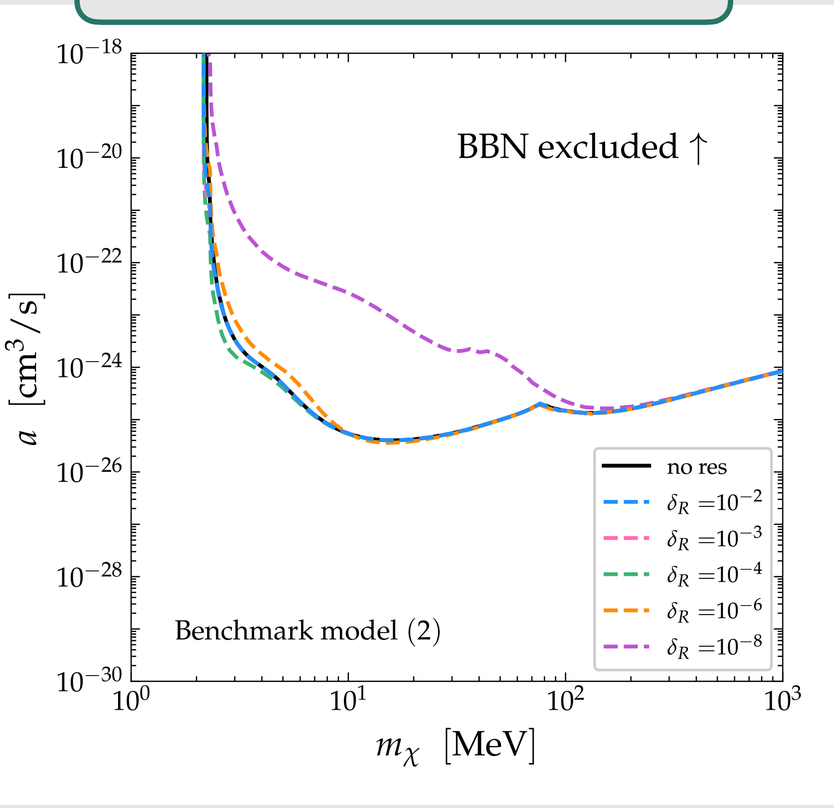
Dynamically determined $T_{\rm kd}$: the resonance is not effective as $T_{\rm kd} \gtrsim 1\,\text{MeV}$

Two scalar model





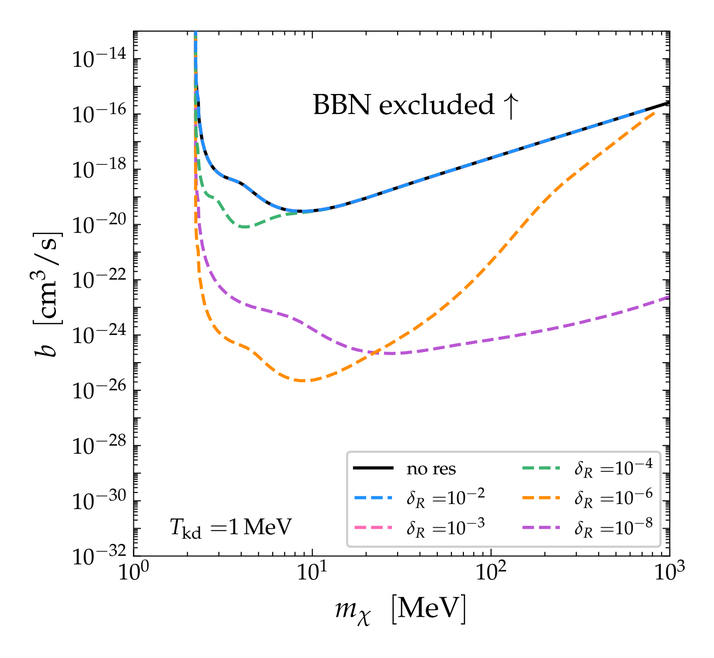
Fermion DM + vector resonance

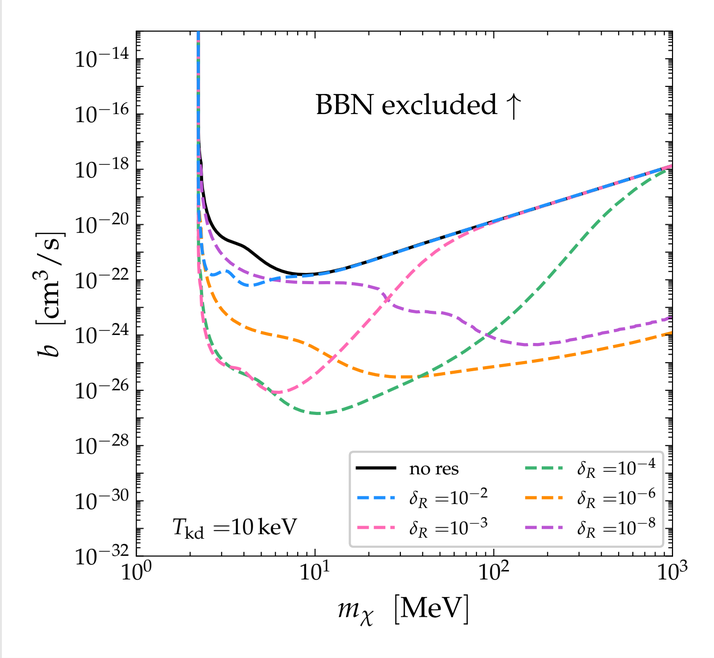


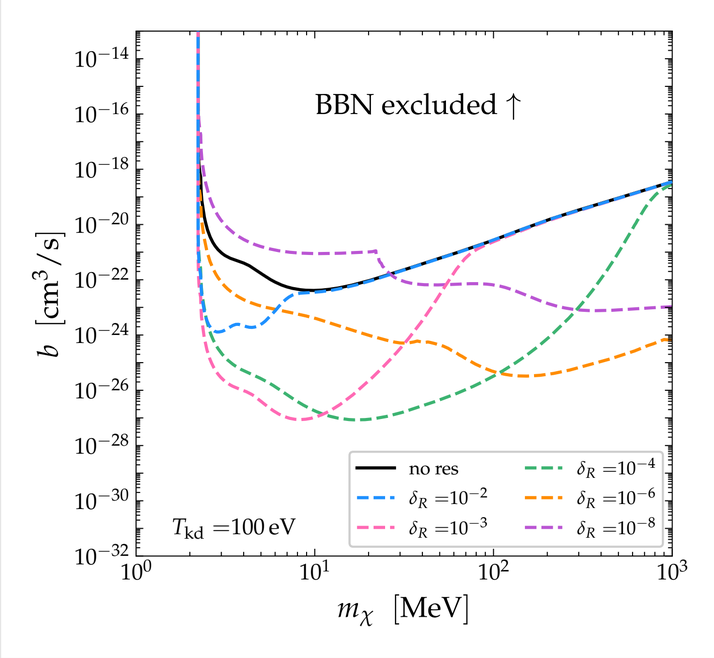
Results (p-wave), fixed $T_{\rm kd}$

$$b = \frac{2\pi\gamma_d\gamma_v}{m_\chi^2\delta_R^2}$$

For p-wave, the resonance effect is typically stronger







Results (p-wave), dynamical $T_{\rm kd}$

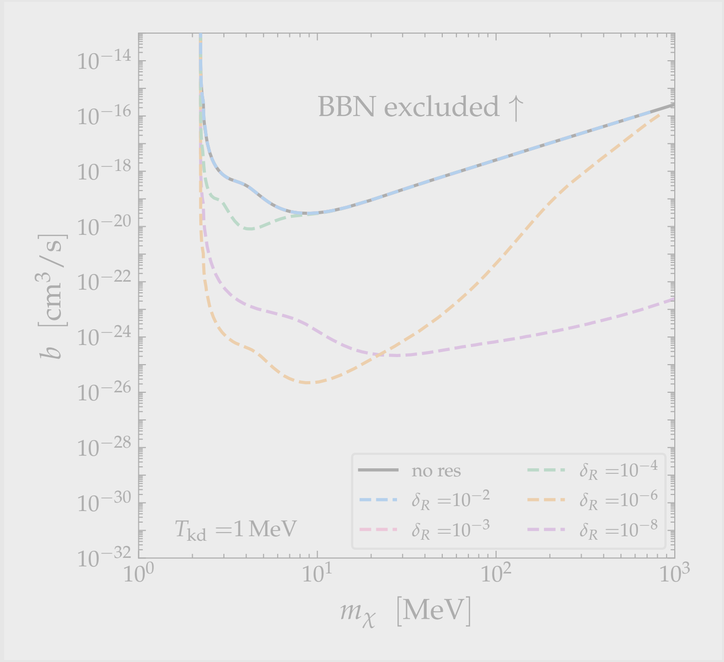
$$b = \frac{2\pi\gamma_d\gamma_v}{m_\chi^2\delta_R^2}$$

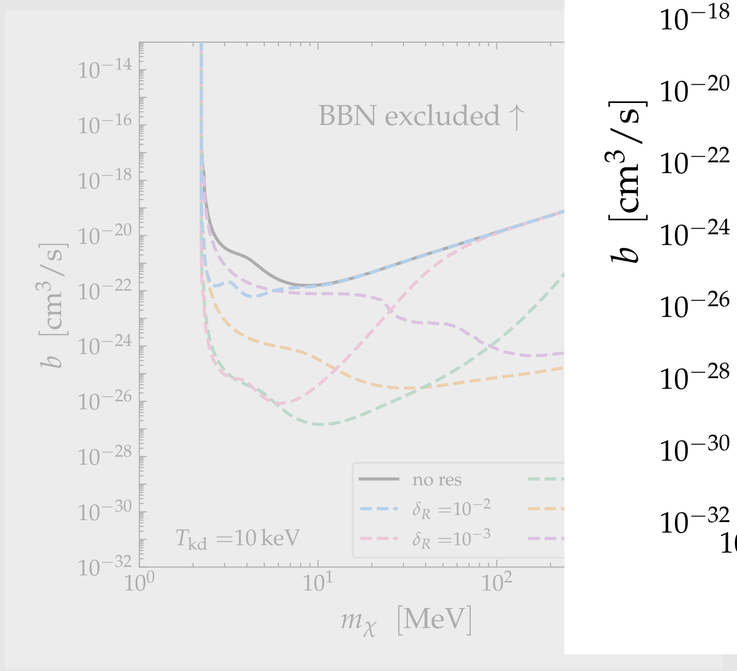
For p-wave, the resonance effect is typically stronger

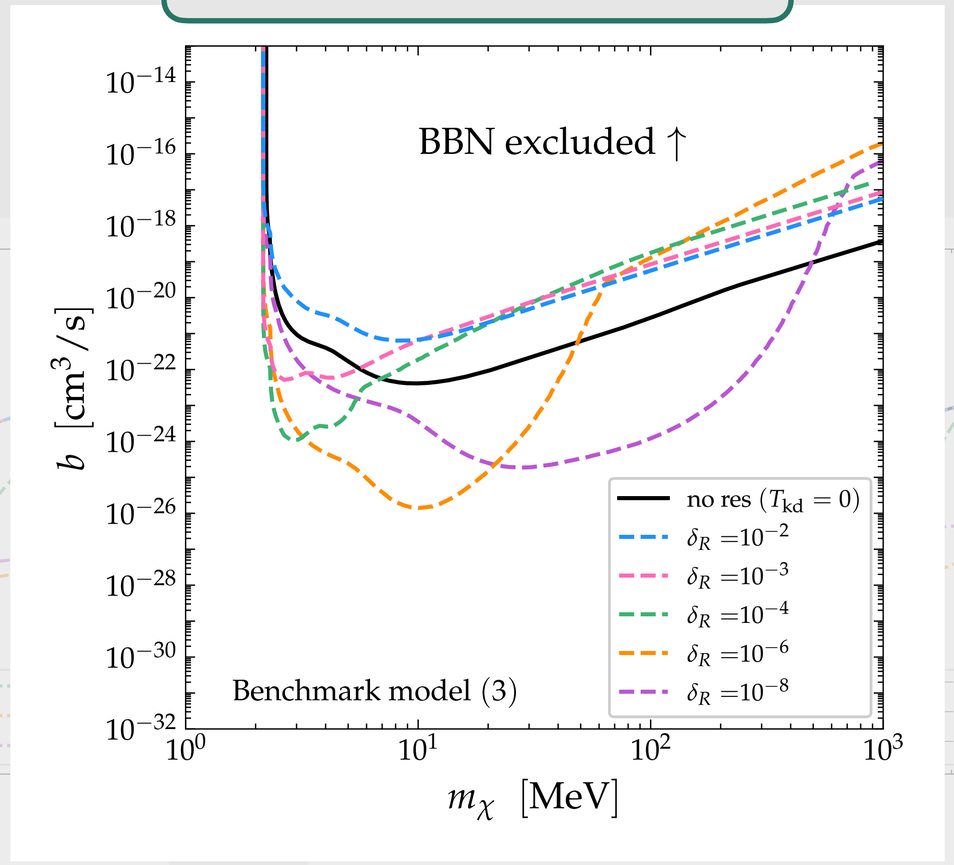
Dynamical $T_{\rm kd}$: resonance models are more strongly constrained compared to vanilla annihilations

Bounds are weaker than s-wave, so later decoupling

Scalar DM + vector resonance







Conclusions

- BBN can place stringent bounds on exotic energy injection in the early universe, such as (resonant) s- or p-wave DM annihilations
- Resonant DM models offer an intriguing solution to the cusp-core problem
- Decoupling temperature greatly impacts the constraints; if in thermal equilibrium long enough, resonance model suffers from stronger bounds*
- *If the resonance is too narrow (i.e. small mass splitting), the bounds can actually get weaker
- Determining the decoupling dynamically for the benchmark models, s-wave resonance does not suffer from increased bounds, whereas p-wave does
- Want to use the code yourself? Will be included in an upcoming version of ACROPOLIS: check the GitHub!


Thank
you!

Back up

Why is the difference between s- and p-wave so pronounced?

Consider the ratio between the resonance contribution and the off-resonance limit at the peak

$$\left.\frac{\langle\sigma_{\rm ann}v\rangle^{\rm res}}{\langle\sigma_{\rm ann}v\rangle^{\rm off-res}}\right|_{x=x_{\rm peak}} \sim \frac{\delta_R^{1/2-n_d}}{\gamma_d} \qquad x_{\rm peak} = \frac{3}{2\delta_R}$$

$$\langle\sigma_{\rm ann}v\rangle^{\rm res} \propto \gamma_v \frac{x^{3/2}}{m_\chi^2} e^{-\delta_R x}, \quad (\gamma_v \ll \gamma_d)$$

$$\langle\sigma_{\rm ann}v\rangle^{\rm off\text{-}res} \propto \frac{\gamma_v\gamma_d}{m_\chi^2\delta_R^2} x^{-n_d}$$

For s-wave ($n_d = 0$), the resonance strength decreases for smaller δ_R, whereas the opposite is true for p-wave ($n_d = 1$)

